nature portfolio

https://doi.org/10.1038/s41586-024-07572-0

Supplementary information

Giant stem tetrapod was apex predator in Gondwanan late Palaeozoic ice age

In the format provided by the authors and unedited

Supplementary Information

Giant stem tetrapod was apex predator in Gondwanan late Palaeozoic ice age

Claudia A. Marsicano, Jason D. Pardo, Roger M.H. Smith, Adriana Mancuso, Leandro Gaetano, and Helke Mocke

Table of Contents

1) Supplementary anatomical figure

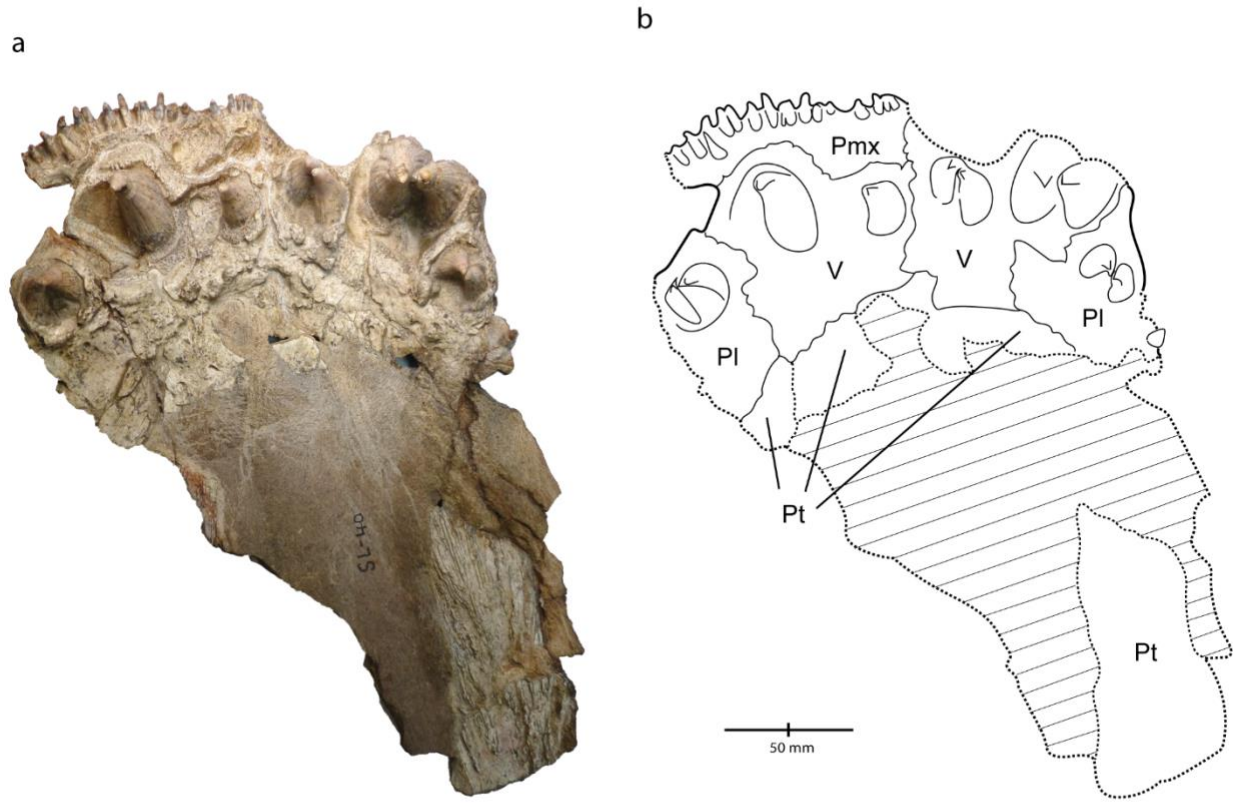

Figure S1. *Gaiasia jennyae* paratype (F-1504). Partial palate showing the arrangement of the palatal tusks and the right premaxilla in position. Pl, palatine; Pmx, premaxilla; Pt, pterygoid; V, vomer. Scale bar 50 mm.

2) Supplementary Data

a) Geological setting and taphonomic notes

i) Tectonic and palaeogeographic setting of Huab Basin

The Gai-As Formation is an argillaceous unit forming the lower half of a ~ 130m thick coarsening-, and progressively shallowing-upwards, fluvio- lacustrine sequence that accumulated at the beginning of the Permian between 280 Ma (Werner, 2006) and 272 Ma ago (Warren et al. 2001; see Supp. Fig. 2A, B). It accumulated within a flooded half-graben (the Huab Basin, Supp, Fig. 3) aligned perpendicular to the eastern margin the major NNE-SSW trending Pre-South Atlantic rift zone (PSARZ) (Stollhofen et al. 2000). Compression generated by the Samfrau active margin to the south caused pulses of uplift and subsidence and long periods of quiescence resulting in multiple hiatuses/disconformities and regional angular unconformities in the sedimentary sequences that filled the peripheral basins (Lambiase 1989; Tankard et al. 1995).

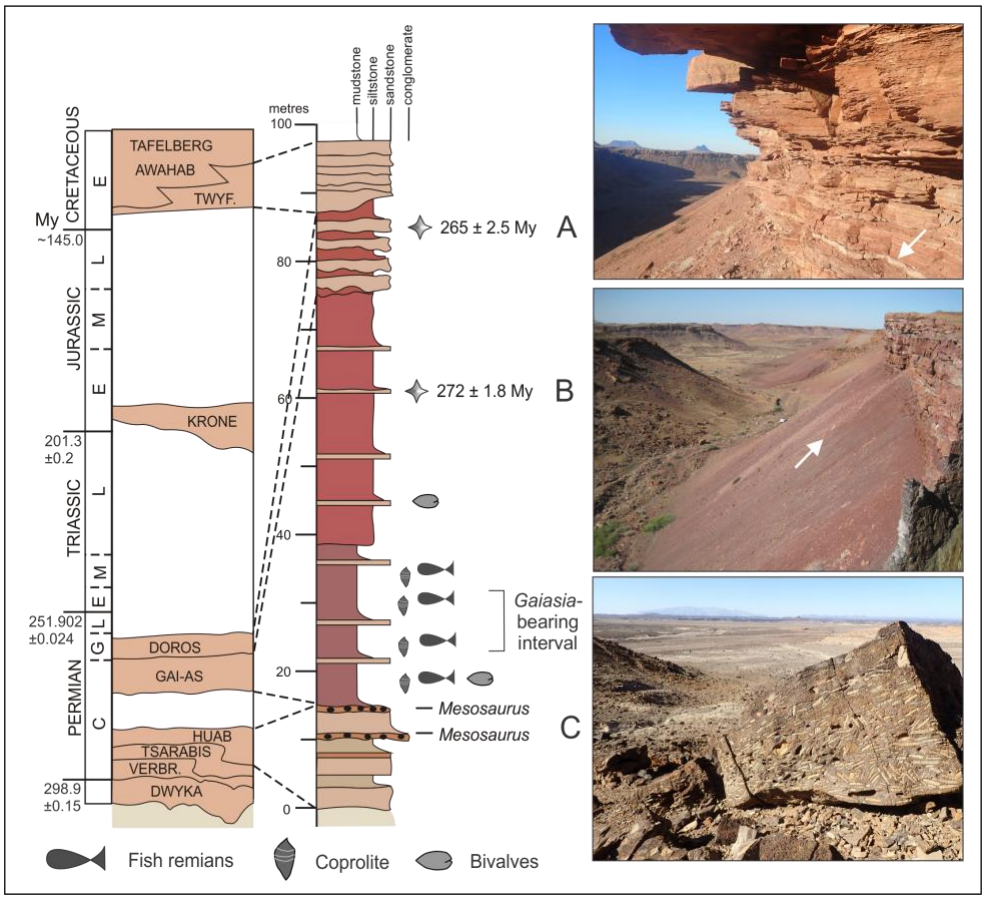

Figure S2. A chronostratigraphic representation of the stratigraphy of the Huab Basin with a more detailed lithological

log of the *Gaiasia* locality showing positions of radiometrically dated tuffs (265+/- 2.5My from Stollhofen et al. 2000; 272+/- 1.8My from Warren et al. 2001) and key fossil-bearing levels. Outcrops images A, B and C are from around the *Gaiasia* locality (north of Doros) and the stratigraphic positions of the dated tuffs are indicated with white arrows.

With waning of the Carboniferous glaciation all the lowland areas of southern western Gondwana became flooded with meltwater, which in early-Permian times (Cisuralian) led to the deposition of the organic-rich Whitehill/Irati Formation mudrocks over large areas on either side of the PSARZ. Today, these *Mesosaurus*-bearing strata, dated at 280.5 Ma (Werner, 2006) and 278.4 Ma (Santos et al. 2006), form a reliable intercontinental biostratigraphic marker and their proximal facies in the Huab Basin (Huab Formation), directly underlies the Gai-As Formation at the *Gaiasia* study site (Supp. Fig. 2C).

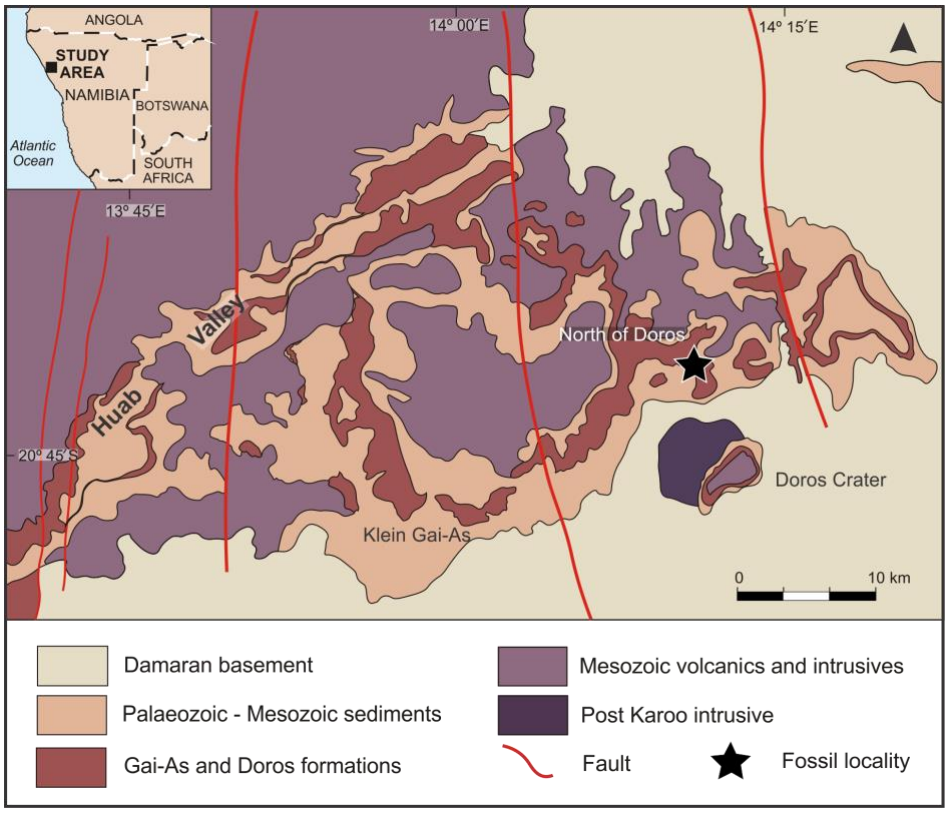

Figure S3. Location map with distribution of the Gai-As and Doros formations and the *Gaiasia* type locality indicated with a star.

The faunal links between the aquatic assemblages of Namibia and Brazil suggest that this elongated inland water body extending over more than 1.5 million km^2 along an overall northwest-southeast trend (Porada et al., 1996). The Gai-As and overlying Doros formations (Supp. Fig. 2B) accumulated in an embayment along the eastern margin of this large lake at around 46.58º S (van Hinsbergen et al., 2015) in a climatic belt that modelers have inferred as cool-temperate and seasonal (Boucot et al. 2013).

ii) Sedimentology of *Gaiasia* locality

The *Gaiasia* specimens and associated fauna were recovered from the lower Gai-As Formation (Supp. Fig. 4A) comprising a 35-m-thick succession of dusky red (2.5 YR 3/2) massive mudstone beds interbedded with weak red (10R4/2) horizontally- and rarely wavy-laminated siltstone. The latter facies contains some 1-3cm thick interbeds of ripple-cross laminated fine- to medium-grained sandstone and rare 10-25cm beds of algally- laminated limestone (Stollhofen et al., 2000). Stollhofen et al. (2000) interpret the depositional environment as the offshore areas of a deep, thermally-stratified, rift valley lake subject to episodic storm-induced turbidity influx and density underflows. However, the presence of *in situ* silicified rhizoliths in association with the calcareous nodule horizons (Supp. Fig. 4B, C) suggests a much shallower-water wetland system with islands of subaerially exposed mudflats that persisted long enough for plants to colonise. At the *Gaiasia* type locality two conspicuous horizons of oblate and commonly elongated, dolomitic concretions (Supp. Fig. 4B) with an external crust of late diagenetic cone-in-cone structured calcite (Supp. Fig. 4C) occur within the fossil-bearing interval. With some measuring up to 3 m in diameter, their formation is clearly micrite precipitation within the sediment pore spaces and appears to be concentrated around thin, silty sandstone lenses some of which contain abundant abraded shark teeth, fish scales, spines, small bones and coprolites (Supp. Fig. 5A–E). These organic-rich sandy lenses are interpreted as storm-generated offshore tempestites (Stollhofen et al. 2000), however, we suggest that they were deposited in a much more proximal setting. At certain times after burial the products of bacterial decomposition of the concentrated organic matter promoted the early

diagenetic precipitation of carbonate from groundwater flowing through the surrounding sediment (Horsthemke, 1992). These precipitation episodes were likely caused by fluctuations in groundwater position and rate of flow through the buried sediments as the lake-margin migrated westwards (Gierlowski-Kordesch, 1998; Williams and Krause, 1998; Alonso-Zarza, 2003).

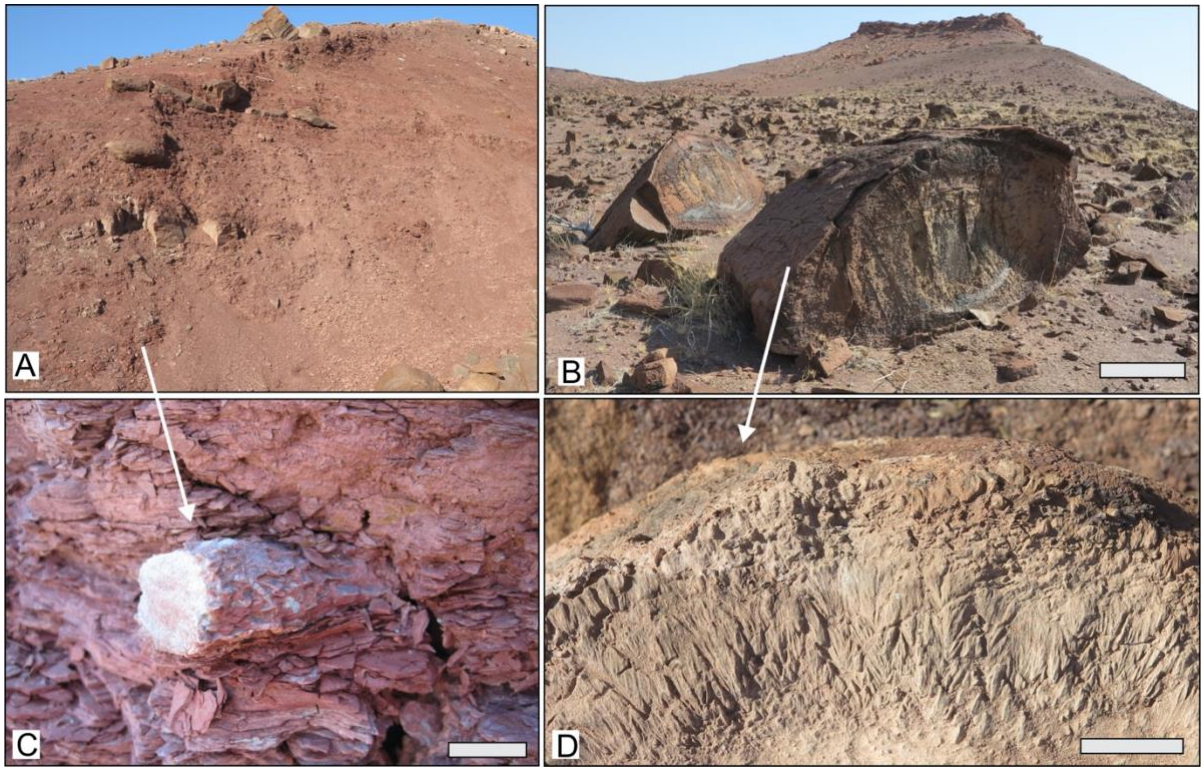

Figure S4. Sedimentological features of Gai-As Fm. A. Lower Gai-As mudrock outcrop showing thin sandstone sheets and large rounded calcareous nodules. B. Large oblate calcareous nodules that have weathered out of the lower Gai-As mudrocks. Some contain isolated temnospondyl bones, fish hash layers, coprolites and non-marine bivalve coquinas. Scale bar = 25 cm. C. A single rhizolith in laminated silty mudstone from the lower Gai-As outcrop. Scale bar = 1cm. D. A crust of cone-in- cone structured calcite completely surrounds some of the large oblate calcareous nodules in the lower Gai-As Formation. Scale bar = 2cm.

iii) The lower Gai-As Formation fossil assemblage

As mentioned earlier, at the *Gaiasia* type locality two closely-spaced horizons of reworked *Mesosaurus* bonebeds occur at the top of the Huab Formation immediately underlying the Gai-As Formation (Supp. Figs. 6A, 5F). They provide a useful intercontinental chrono-stratigraphic marker for the early Permian and have been radiometrically-dated as late Cisuralian, Artinskian/Kungurian in age. There follows a definite hiatus but of unknown duration before the first Gia-As sedimentation began (Wanke et al., 2000). The lowermost Gai-As fossils recovered are isolated temnospondyl vertebrae, fish teeth (Supp. Fig. 5A), fish spines (Supp. Fig. 5B) and scale-filled coprolites (Supp. Fig. 5D). A horizon some 5 m above base is where lenticular coquinas of locally-concentrated non-marine bivalves are commonly found inside thinly-laminated micrite nodules (Supp. Fig. 5E). From around 5-15m above the base, isolated elements, partially articulated and fully-articulated temnospondyl and rare fully articulated fish skeletons (Supp. Fig. 5C) occur within elongate calcareous nodules along with scale-bearing and non-scale-bearing coprolites. This is the *Gaiasia*-bearing interval (see Supp. Fig. 2).

iv) Taphonomic description of *Gaiasia* specimens

The *Gaiasia* type specimen (F-1528) comprising the skull with articulated lower jaw and fully-articulated partial axial skeleton was preserved dorsal-up and completely enveloped with calcareous nodular material. It was found *ex-situ*, in 5 separate blocks (Supp. Fig. 6B) that had apparently sequentially weathered-out of the red mudrocks and fallen down a 45º slope (Supp. Fig. 6C). All the blocks fitted together leaving only the rear end of the skeleton, approximately just anterior to the sacrum to the tip of the tail, still missing. The large skull block was at the top of the bone train and it is likely that its flattened shape prevented it rolling downslope, thus remaining closest to the original stratigraphic level. A second near complete skull of the same taxon (F-1522) was found *in situ* in the adjacent valley (Supp. Fig. 6A, C). This too was encrusted with nodular micrite and lying dorsal-up. It was excavated from massive pale-red siltstone at almost the same stratigraphic level as the skull F-1528 confirming that this is the *Gaiasia*-bearing interval.

Figure S5. Associated fauna. A. Close up of a xenacanthid shark teeth in a micro-bonebed within a large calcareous nodule. Scale bar = 2cm. B. Portion of shark spine. Scale bar = 1 cm. C. Complete actinopterigian fish in calcareous nodule. Hammer length = 32.5 cm. D. Selection of scale-bearing coprolites from the Lower Gai-As Formation. Scale bar = 5 cm. E. Coquina of non-marine bivalves within a large elongate calcareous nodule in the lower of the two horizons of large nodules encountered in the Lower Gai-As succession. Scale bar = 2cm. F. Reworked *Mesosaurus* post-crania in a bonebed at the top of the Huab Formation. This unconformably underlies the Gai-As Formation at the *Gaiasia* locality with a hiatus of unknown duration. Scale bar = 1cm.

On preparation of the specimens, it was discovered that both skulls had suffered considerable vertical compression that had occurred after burial and before micrite peri-mineralization. The skulls are deeply indented in all the parts that are not directly supported from beneath (Supp. Fig. 6D). In the process of collapse, the weakly sutured dermal elements of the skull roof were forced apart. With no evidence of bone breakage, or sub aerial-weathering, it appears that these two specimens were buried in a low-energy subaqueous environment. However, the overall cranial and postcranial anatomy and the dental morphology suggest *Gaiasia* as a bottom-dwelling ambush predator that would have been best accommodated a relatively shallow-water wetland habitat in a more marginal setting rather than the previously interpreted offshore deep lake bed. If the lower Gai-As Formation is an offshore deposit then the most plausible taphonomic pathway for the articulated *Gaiasia* skeletons is that the "bloat and float" scenario whereby floating carcasses were blown offshore and settled through the stratified water column into the muddy bottom when the stomach gasses escaped (*cf.* Schafer 1972). Evidence contrary to this interpretation is that the calcareous nodule formed around both articulated *Gaiasia* specimens is notably thicker on the lower side than the top (Supp. Fig. 6B). Thus, even though the second specimen was found *ex situ*, we are confident that both carcasses were buried in a dorsal-up attitude, and as such they do not support the bloat-and-float pathway which invariably leads to ventral-up preservation. Thus, we prefer the simpler scenario that the articulated skeletons were buried quickly, soon after death in their natural habitat, by fluvially-sourced sediment plumes that periodically inundated the wetlands that flanked the margins of a deep water lake.

Figure S6. *Gaiasia* taphonomy. A. Panorama of *Gaiasia* excavation with the outcrop of the *Mesosaurus*-bearing Huab conglomerates indicated with white arrows. B. Reassembling the *ex situ* type specimen of *Gaiasia jennyae* (F 1528)– a dorsal up skull with lower jaw and most of the articulated axial skeleton. C. *In situ* dorsal-up *Gaiasia jennyae* skull (F 1522) at locality shown in A. panorama. D. Type specimen of *Gaiasia jennyae* (F 1528) shown in B. after preparation. Note the differential compression of the skull roof. There is no evidence of pre-burial breakage or subaerial weathering. Scale bar =10cm.

b) Character list

A new data set was constructed by a combination of characters from previous comprehensive analyses on basal tetrapods, some of them modified, and new characters produced during the present work.

Skull

1. Orbit location: about halfway along the skull table length [0]; in front of the mid-length of the skull [1]; behind mid-length of the skull [2]. (Warren & Marsicano, 2000).
2. Interorbital distance: less than 25% of the width of the skull at midorbital level [0]; greater than 25% of the width of the skull at midorbital level [1]. (Yates & Warren, 2000).
3. Skull margins: straight or slightly concave when see from above [0]; slightly convex [1]. (Yates & Warren, 2000).
4. Contour of the cheek in occipital view: slightly convex [0]; straight [1]. (Yates & Warren, 2000).
5. Length of the posterior skull table (length measured as the sagittal distance from the level of the posterior edge of the orbits to the posterior margin of the skull roof; width measured as the width from the lateral edge of one tabular to the other): between 70% and 90% of its width [0]; length of the posterior skull table 50–65% of the width [1]; length of posterior skull table less than 46% of the width [2]; length of posterior skull table greater than 90% of the width [3]. (Yates & Warren, 2000).
6. Sculpture of the dorsal skull roof: forms a 'normal' ridge-grooved pattern without pustules or nodules on the junctions [0]; spider-web pattern with pustules or nodules on the junctions of crests and ridges [1]; only pustules are present [2]. (Marsicano & Warren 1998).
7. Zones of subdued ornamentation in the skull table: present [0]; absent [1]. (Milner & Sequeira, 1994, 1998).
8. Nares location: not close to skull midline (distance between nares twice width of one naris or

greater) [0]; nares close to skull midline (distance between nares approximates width of one naris) [1]. (Warren & Marsicano, 2000).

9. Nares shape: rounded [0]; narrow and anteroposteriorly elongated [1]; pear-shaped so they narrow anteriorly [2].
10. Prenarial snout formed by an anterior expansion of the premaxilla: present [0]; absent [1]. (Holmes et al., 1998).
11. Prenarial skull length: less than internarial distance [0]; equal to or up to three times the internarial distance [1]; greater than three times the internarial distance [2]. (Yates & Warren, 2000).
12. Snout margins: continually converging towards the tip [0]; tip of snout expanded so that the snout margins are parallel, or snout margins concave before the tip [1]. (Yates & Warren, 2000).
13. Sensory sulci: well developed [0]; present but poorly developed [1]; deeply incised between orbit and nostril only [2]; absent [3]. (Warren & Marsicano, 2000).
14. Premaxilla with a triangular posterior process (= alar process Milner & Sequeira, 1994; Holmes et al., 1998): present medial to the naris [0]; triangular process absent and the posterior dorsal margin of the premaxilla forms a simple suture with the nasal [1].
15. Premaxilla lateral margin: medial margin only slightly shorter than its lateral margin [0]; premaxilla shows a conspicuous elongation along its lateral margin but not medially thus the interpremaxillary suture is less than half as long as its lateral margin [1]. (Milner and Sequeira, 1994).
16. Internarial fenestra in the junction between the premaxillae and nasals: present [0]; absent [1]. (Yates & Warren, 2000).
17. Contact between premaxilla and nasal: anterior to the nares [0]; at level of the nares [1]; posterior to the nares [2].
18. Septomaxilla: part of the skull roof forming the posterior nasal margin [0]; part of the skull roof

and with a well-developed intranarial process [1]; restricted to the floor of the nasal cavity with limited or no contact with the posterior nasal margin [2]; unossified [3]. (modified from Yates & Warren, 2000).

19. Lacrimal: present [0]; absent [1]. (Milner, 1990).
20. Lateral border of the orbits: formed only by the lacrimal and jugal (0); lateral edge of the corpus of the palatine exposed dorsally in the lateral margin of the orbit (LEP "lateral exposure of the palatine") [1]; external border formed by prefrontal-jugal contact [2]; lateral border formed exclusively by the lacrimal and postorbital [3] (Milner, 1990; Holmes et al., 1998).
21. Jugal: extends anterior to anterior orbital margin [0]; anterior end of jugal about level with or posterior to anterior orbital margin [1]. (Warren & Marsicano, 2000).
22. Prefrontal and jugal: not in contact [0]; form a nearly straight suture anterior to the orbit [1]; long and stepped jugal-prefrontal contact anterior to the orbit [2]. (modified from Yates & Warren, 2000).
23. Prefrontal: does not contribute to the margin of the external naris [0]; contributes to the margin of the external naris [1]. (Yates & Warren, 2000).
24. Prefrontal shape: crescent-shaped and curves around the anteromedial border of the orbit [0]; anteroposteriorly elongated prefrontal located between the nares and orbits [1].
25. Prefrontal-maxilla contact: absent [0]; present [1].
26. Prefrontal-postfrontal contact: present [0]; prefrontals and postfrontals fail to contact so that the frontal contributes to the orbital margin [1].
27. Prefrontal-postfrontal suture location: anterior to the midpoint of the orbit [0]; situated approximately at or posterior to the midpoint of the orbit [1]. (modified from Sequeira, 2004).
28. Postorbital shape: anteroposteriorly elongated tapering in a pointed, subtriangular posterior process [0]; quadrangular or rounded but not tapering in a pointed, subtriangular posterior process [1]; postorbital L-shaped ("hooked" sensu Damiani 2001) [2]. (Sequeira, 2004; Ruta & Bolt, 2006)

29. Postorbital-orbit: postorbital not wider than the orbit [0]; wider [1]. (Ruta & Bolt, 2006).
30. Length of the suture between the postorbital and the jugal: less than half of the maximum length of the postorbital [0]; more than half of the maximum length of the postorbital [1]. (Ruta & Bolt, 2006).
31. Prefrontal-nasal relative size: prefrontal anteroposteriorly longer or subequal than nasal [0]; prefrontal shorter than nasal [1].
32. Postfrontal-postorbital relative size: postfrontal anteroposteriorly longer or subequal than postorbital [0]; postfrontal shorter than postorbital [1].
33. Frontal length: shorter than the parietal [0]; longer than the parietal [1]; subequal to the parietal [2].
34. Anterior margins of the frontals: not wedged between the posterolateral margins of the nasals for at least one-third of their maximum length [0]; wedged between the posterolateral margins of the nasals for at least one-third of their maximum length [1]. (Ruta & Bolt, 2006).
35. Intertemporal: present [0]; absent [1] (Milner & Sequeira, 1994; Holmes et al., 1998).
36. Maxilla and nasal: not in contact [0]; maxilla and nasal form a suture [1].
37. Maxilla and quadratojugal: form a suture or a point contact on the ventral border of the cheek [0]; maxilla and quadratojugal do not contact [1]. (Yates & Warren, 2000).
38. Maxilla: extending posterior to the level of the posterior margin of the orbit [0]; terminating at the level of such margin or anterior to it [1]. (Ruta & Bolt, 2006).
39. Inward inflection of skull outline in dorsal view at the level of the maxilla-premaxilla suture: absent [0]; present [1]. (Ruta & Bolt, 2006).
40. Maxilla-orbit: maxilla not contributing to the margin of the orbit [0]; contributing [1]. (Ruta & Bolt, 2006).
41. Anteroposterior length of the supratemporal: shorter than the length of the squamosal [0]; as long as the squamosal [1].
42. Parietal bones: project posterolaterally (L-shaped) [0]; parietals quadrangular [1].

43. Anteriormost extension of the external surface of the squamosal: lying posterior to the parietal midlength [0]; in front [1]; approximately level with the parietal midlength [2].
44. Parietal-postorbital contact: absent [0]; present [1].
45. Combined transverse width of the postparietals: less than four times the anteroposterior length of the postparietal [0]; combined transverse width greater than four times the length [1].
46. Length of parietal: more than two and a half times its width [0]; parietal less than two and a half times long as wide [1].
47. Combined width of both parietals: approximately equal to the interorbital width [0]; smaller than the interorbital width [1]; larger than interorbital width [2].
48. Maximum width of the parietal: greater than that of the supratemporal [0]; subequal to that of the supratemporal [1]; less than that of the supratemporal [2].
49. Pineal foramen: present [1]; absent [1]. (Milner & Sequeira, 1994, 1998).
50. Position of the pineal foramen: posterior to the interparietal suture mid length [0]; approximately level with [1]; anterior to the interparietal suture mid length [2]. (Ruta & Bolt, 2006).
51. Postparietals: do not taper abruptly laterally [0]; tapering [1].
52. Postparietal-supratemporal contact: do not form an L-shaped ("stepped") suture [0]; postparietals do form an L-shaped ("stepped") suture with the supratemporals [1]; postparietal-supratemporal contact absent [2].
53. Tabulars: well developed rectangular to triangular bones [0]; reduced to thin slivers lying against the posterior margin of the skull roof [1].
54. Tabular horns end: at the same level as or anterior to the posterolateral corners of the skull roof [0]; tabular horns extend posterior to the posterolateral corners of the skull roof [1].
55. Tabular horn: posteriorly directed [0]; laterally directed towards the squamosal thus partly enclosing the otic notch [1].
56. Maximum length of the dorsal ornamented surface of the tabular: greater than one-third of the maximum length of the postparietal [0]; less than or equal to one-third of the maximum length

of the postparietal [1].

57. Otic notch: deep [0]; as a wide shallow embayment [1]; absent [2].
58. Deep otic notch: with its anterior end surpassing anteriorly the tabular bones [0]; anterior end of the otic notch behind the anterior border of the tabulars [1].
59. Squamosal-tabular contact: separated by the supratemporal [0]; squamosal-tabular suture present on the dorsal skull roof [1]. (Boy, 1990; Holmes et al., 1998).
60. Post postparietal process of the skull roof: absent [0]; present [1].
61. Occipital condyles: do not project beyond the posterior margin of the skull table [0]; condyles well projected beyond the posterior margin of the skull table producing an anteriorly inclined occiput [1]; condyles at approximately the same level or somewhat projected from the posterior margin of the skull table, but no producing and anteriorly inclined occiput [2]. (modified from Warren & Marsicano, 2000).
62. Quadrate condyle position: well posterior to the occipital condyles [0]; in approximately the same transverse plane as the occipital condyles [1]; anterior to the occipital condyles [2].
63. Occipital condyle: single with the basioccipital contributing in the articulating surface [0]; bilobed occipital condyle with reduced basioccipital contribution [1]; double occipital condyles (exoccipital) with no basioccipital contribution [2]. (Milner, 1990).
64. Quadratojugal: forms a simple corner with the quadrate in occipital view [0]; a sulcus present on the quadratojugal lateral to the quadrate condyles, so that the quadratojugal forms an overhang in occipital view [1]. (Yates and Warren; 2000).
65. Paraquadrate foramen: present on the occipital portion of the quadratojugal [0]; present on posteroventrolateral ornamented portion of quadratojugal [1]; absent [2].
66. Ascending ramus of the pterygoid: contacts dorsolaterally with the squamosal [0]; does not contact the squamosal creating an upper palatoquadrate fissure [1]. (Warren & Black, 1985).
67. Ascending ramus of the pterygoid: forms a continuous curve with the posterior edge of the quadrate ramus [0]; arises abruptly from the dorsal surface of the pterygoid [1].

68. Posterior face of quadrate ramus of the pterygoid: lacking an oblique ridge [0]; a large, sharp lamina (oblique ridge) rises vertically from the occipital surface of the quadrate ramus at the level of the dorsalmost tip of the quadrate when see from behind and partially conceals the ascending ramus in occipital view [1]; the oblique ridge is a relatively low lamina that does not conceal the ascending ramus from behind [2]. (see Marsicano et al., 2017).
69. Quadrate ramus of the pterygoid: level with palate [0]; quadrate ramus slightly downturned [1]; quadrate ramus strongly downturned [2]. (modified from Warren & Black, 1985).
70. Occipital face of the quadrate: with a boss medially, close to its suture with the pterygoid ("tuberculum hyoideus" sensu Shishkin, 1973; "boss" sensu Watson 1962) and it is located at the same level where the ledge of the quadrate ramus of the pterygoid rises when present [0]; boss absent [1].
71. Foramen passing though the stapes: present [0]; absent [1].
72. Post temporal fenestra: markedly wider than deep [0]; about as wide as deep or deeper than wide [1]; post temporal fenestra reduced to small foramen or entirely closed [2]; post temporal fenestra slit-shaped [3]. (Marsicano et al., 2017).
73. Paroccipital process: nearly parallel to the skull roof [0]; at approx. 45 degrees angle to the skull roof [1].
74. Paroccipital process shape: approximately rod-like in cross section [0]; ventrally projected as a thin lamina along its length that partially conceals the pterygoid from behind [1]; the lamina is more developed distally, under the tip of the tabular horn, thus forming a prominent ventral flange [2]. (Marsicano et al., 2017).
75. Paroccipital process: extends slightly beyond the tip of the tabular horn thus an unornamented process is developed just below the distal end of the horn [0]; unornamented process absent [1]. (Marsicano et al., 2017).
76. Supraoccipital: absent [0]; present [1]. (Schoch, 2013; Pardo el al., 2017a).
77. Basioccipital (length): anteriorly extended towards the basisphenoid [0]; foreshortened to a

narrow posterior rim [1]. (Schoch, 2013; Pardo el al., 2017a).

78. Ossified opisthotic: present [0]; absent [1].
79. *Excavatio tympanica* on the medial surface of the ascending ramus of the pterygoid, just behind the basipterygoid articulation: absent [0]; present [1]. (Bystrow & Efremov, 1940; Romer & Witter, 1942).
80. Ceratobranchials in adults: absent or unossified [0]; present [1]. (Witzmann, 2013).
81. Basibrachial in adults: absent or unossified [0]; present [1]. (Witzmann, 2013).
82. Anterior palatal opening: not perforated [0]; anterior palatal opening perforated to form an single anterior palatal vacuity [1]; anterior palatal opening perforated to form a paired anterior palatal vacuity [2]; absent [3]. (modified from Yates & Warren, 2000).
83. Choana: rounded to oval [0]; slit-like [1].
84. Palatal surface of the premaxillae: absence of a medial tubercle [0]; a rugose, medial tubercle located on the suture between the premaxillae (=*tuberculum subrostrale medium*, Gubin 1986; =premaxillary tubercle, Holmes 2000) [1].
85. Lateral border of choana: form mostly by the maxilla [0]; lateral processes of vomer and palatine approach one another so as to reduce the maxillary contribution [1]; vomer-palatine suture lateral to the choanae excludes maxilla entirely [2]; form by premaxilla and maxilla [3].
86. Maxilla-vomer contact: absent or in point contact [0]; maxilla and vomer forming a suture [1].
87. Palatine ramus of the pterygoid: contacts the vomer on the anterior edge of the interpterygoid vacuity thus preventing its exposure on the border of the vacuity [0]; palatine ramus of the pterygoid contacts the vomer on the anterolateral border of the interpterygoid vacuity leaving a small exposure of the vomer on the border [1]; palatine ramus of the pterygoid not in contact with the vomer [2]. (modified from Milner, 1990; Milner & Sequeira, 1994).
88. Vomerine ridges radiating towards the margins of the snout from a centre near the anteromesial corner of the choanae: absent [0]; present [1]. (Sequeira, 2004; Ruta & Bolt, 2006).
89. Palatine ramus of the pterygoid: meets palatine on the lateral margin of interpterygoid vacuity

[0]; pterygoid retracted so ectopterygoid is exposed in the interpterygoid vacuity [1]; pterygoid markedly retracted so ectopterygoid makes a large contribution to strut between interpterygoid and subtemporal vacuities [2].

90. Posterolateral flange on the palatine ramus of the pterygoid: present [0]; flange absent [1].
91. Pterygoid palatal rami meet anteriorly on the midline of the palate: present [0]; absent [1].
92. Posterior edge of the ectopterygoid: contributes to the anterior margin of the subtemporal fossa [0]; posterior end of the ectopterygoid separated from the subtemporal fossa by a jugal-pterygoid contact [1]. (Holmes et al., 1998; Ruta & Bolt, 2006).
93. Interpterygoid vacuities: present [0]; absent [1]. (Holmes et al., 1998; Ruta & Bolt, 2006).
94. Maximum width of the interpterygoid vacuities: anterior to the midpoint of the vacuity [0]; approximately at mid-length of the vacuity [1]; posterior to the midpoint of the vacuity [2].
95. Interpterygoid vacuities occupying at least half of the maximum palatal width (not including the width of the intervening cultriform process of the parasphenoid): absent [0]; present [1]. (Ruta & Bolt, 2006).
96. Margins of the palatal bones delimiting the interpterygoid vacuities: straight or partially concave [0]; concave along their whole length [1]. (Ruta & Bolt, 2006).
97. Parasphenoid basal plate: articulates with depressions in the corpus of the pterygoid [0]; an elongate cylindrical to hemicylindrical medial process of the pterygoid abuts the parasphenoid [1]; corpus of the pterygoid forming a flat suture (basicranial suture) with the parasphenoid plate [2]. (Yates & Warren, 2000; Schoch, 2013).
98. Internal carotid artery: entered basicranium ventrally at the level or in front the basicranial joint [0], or at posterolateral corners of the parasphenoid plate, posterior to the basicranial join [1]; internal carotids deeply embedded in the parasphenoid thus branches passing along the dorsal surface of the parasphenoid plate [2]. (Yates & Warren, 2000).
99. Outline of the parasphenoid plate: subrectangular, longer than wide [0]; parasphenoid plate slightly wider than long or as wide as long [1]; parasphenoid plate expanded transversely

creating lateral ‘wings’ [2].

100. Broad embayment along the posterolateral margins of the parasphenoid plate, extending anteroposteriorly for at least one-third of the length of the parasphenoid plate: absent [0]; present [1]. (Ruta & Bolt, 2006).

101. Elongate grooves flanked by distinct ridges that run anteroposteriorly to posterolaterally on the ventral surface of the parasphenoid plate from a point situated behind the basipterygoid processes to a posterolateral notch visible along the lateral margin of the plate: absent [0]; present [1]. (Ruta & Bolt, 2006).

102. Pterygoid: contact only the parasphenoid at the level of the basicranial suture [0]; aditionally also contact the basioccipital and/or the exoccipital [1].

103. Crista muscularis of parasphenoid: present at the level of the basicranial contact [0]; present behind the level of the basicranial contact [1]; crista muscularis absent [2].

104. Ventral surface of the parasphenoid: without sharp rimmed depressions ("pockets" sensu Watson, 1962) [0]; depressions situated on ventral surface of the corpus of the parasphenoid [1]; excavated on the corpus of the parasphenoid so that they are situated dorsally to the ventral surface of the bone [2]. (Marsicano et al., 2017)

105. Width of the cultriform process of the parasphenoid at its midpoint: less than 10% of the length of the process (length of the cultriform process measured as the length between the anterior and posterior ends of the interpterygoid vacuities) [0]; width of cultriform process more than 10% of its length [1]. (Yates & Warren, 2000).

106. Cultriform process of the parasphenoid: projects anteriorly between the vomers beyond the anterior border of the interpterygoid vacuities [0]; cultriform process ends at the level of or behind the anterior border of the interpterygoid vacuities [1].

107. Expansion at the base of the parasphenoid cultriform process: absence [0]; presence [1]. (Ruta & Bolt, 2006).

108. Vomerine depression or foramen just anterior to cultriform process of the parasphenoid: absent

[0]; present [1]; present as a vacuity [2].

109. Prefenestral division of the palate (vomerine plate anterior to the interpterygoid vacuities): wider than long [0]; longer than wide [1]; approximately as wide as long [2]. (Damiani, 2001).

110. Posterior extension of the vomer: present on the lateral border of the interpterygoid vacuity until the level of the palatine fangs [0]; posterior extension of the vomer absent [1].

111. Posteromedial corner of the palatine: simple not extending posterior to the most anterior ectopterygoid tooth [0]; elongate posteromedial process of the palatine extending posterior to the most anterior ectopterygoid tooth [1].

112. Ectopterygoid vs. Palatine: ectopterigoid longer than or as long as palatine [0]; shorter than the palatine [1]. (Ruta & Bolt, 2006).

113. Palatal and quadrate ramus of the pterygoid: well differentiated from one another at the level of the pterygoid corpus [0]; palatal and quadrate ramus of the pterygoid poorly differentiated and forming a continuous sheet of bone on the medial border of the subtemporal vacuity [1]. (Warren & Marsicano, 2000).

114. Posterior edge of the pterygoid: incised close to the suture with the parasphenoid, [0]; not incised [1].

115. Basioccipital-pterygoid contact: absent [0]; present [1].

116. Ventral surface of the pterygoids: without ornament [0]; with ornament [1].

117. Ventral surface of the parasphenoid corpus: without ornament [0]; with ornament [1].

118. Tooth shape: more or less rounded in cross section close to their base [0]; teeth compressed and labiolingually elongated in cross section [1].

119. Conspicuous caniniform region in marginal dentition that involves one or more enlarge (50% or more) teeth: absent [0]; present [1]. (Milner & Sequeira, 1998; Ruta & Bolt, 2006).

120. Medial margin of the choana: without teeth [0]; medial margin of the choana with a row of teeth [1].

121. Vomer tooth row: without a row of teeth between the vomerine fangs [0]; with a tooth row

running transversely between the vomerine fangs [1].

122. Vomerine fangs: absent [0]; a pair of fangs is present between the choanae [1]; two pair of fangs on each vomer [2]. The term fangs is employed here to identify teeth in which the basal diameter and/or height are 25% greater in maximum basal diameter and/or height than the average size of the adjacent marginal premaxillary or maxillary teeth (definition from Ruta & Bolt, 2006).

123. Vomer denticles: continuous field of denticles on the vomers [0]; field of denticles in defined raised symmetrical patches [1]; denticles in a continuous raised area over the vomers [2]; vomers without a field of denticles [3]. (Marsicano, et al., 2017).

124. Palatine fangs: present [0]; absent [1]. (Ruta & Bolt, 2006).

125. Palatine denticles: present [0]; absent [1].

126. Palatine tooth row: absence of a tooth row behind the palatine tusks [0]; four to six palatine teeth [1]; more than seven palatine teeth [2].

127. Ectopterygoid tusks: present on its anterior end [0]; ectopterygoid tusks absent [1].

128. Ectopterygoid teeth: with only one or two teeth [0]; with a tooth row of more than three teeth [1]; ectopterygoid with two rows of teeth [2]; ectopterygoid without teeth [3]. (Marsicano et al., 2017).

129. Pterygoid denticles: absent [0]; pterygoids covered by denticles [1].

130. Relationship of nares to oral margin: nares directly adjacent to oral margin [0]; nares separated from oral margin by well-developed contact between premaxilla and maxilla [1]. (Pardo et al., 2017a).

131. Medial border of nares: nares bordered medially by anterior tectal bone [0]; nares bordered medially by nasal or alary process of premaxilla [1]. (Pardo et al., 2017a).

132. Palatal shelf of premaxilla: absent, premaxilla restricted to tooth row in palatal aspect [0]; broad medial shelf of premaxilla between tooth row and vomer [1]. (Pardo et al., 2017a).

133. Occipital articulation with large notochordal component: present [0]; absent [1]. (Pardo et al.,

2017a).

134. Passage of occipital artery: enters the calvarium through a large foramen[0]; does not enter the space between calvarium and neurocranium [1]. Comment: A prominent foramen on the occipital surface has been associated with the passage of the occipital artery in many stem Tetrapoda (Clack 2003). This passage is seemingly homologous with the fossa bridgei of early osteichthyans, including tetrapodamorph sarcopterygians, although the latter is laterally positioned and enters the space between the otic capsule and calvarium laterally within the medial wall of the spiracle. The plesiomorphic state of this character corresponds to either condition, whereas the derived state is restricted to forms where the occipital artery does not enter the skull (Pardo et al., 2017b).

135. Metoptic foramen (Vagus+Jugular foramen): passes between opisthotic and occipital arch [0]; passes through exoccipital [1]. (Pardo et al., 2017a).

136. Preopercular bone: present [0]; absent [1].

137. Extent of parasphenoid: restricted to cultriform process [0]; it covers the ventral surface of prootics only [1]; covers the ventral surface of entire otic and sometimes occipital region [2]. (Pardo et al., 2017a).

138. Basal tuberosities on ventral surface of otic region: present [0]; absent [1]. Comment: This character refers to fully endochondral structures of the otoccipital region, posteromedial to the fenestra vestibularis. This is distinct from parasphenoid pockets accommodating hypaxial musculature. For a full discussion of this character, see Pardo et al. (2017b)

139. Parasphenoid pierced by buccohypophyseal foramen: present [0]; absent [1].

140. Width of palatine and ectopterygoid: essentially limited to tooth row [0]; with broad medial shelf between tooth row and pterygoid [1]. (Pardo et al., 2017b).

141. General construction of palatoquadrate: *columella cranii* continuous with ascending ramus of pterygoid [0]; *columella cranii* separated from ascending ramus of pterygoid by U-shaped recess more than 1/3 height of the pterygoid, resulting in a distinct epipterygoid element [1].

(Pardo et al., 2017b).

142. Epipterygoid, if present: large platelike element tightly associated with pterygoid [0]; slender element [1]; transversely expanded along anterior margin of palatal ramus [2]. (Pardo et al., 2017b).

Mandible

143. Extension of the mandible behind the glenoid fossa (PGA, Post Glenoid Area, Jupp & Warren, 1986): absent [0]; a relatively short PGA present, approx. as long as the glenoid [1]; a well-developed PGA present, much longer than the glenoid fossa when seen from above [2].

144. Postglenoid process labially on the posterior end of the surangular behind the glenoid: absent [0]; postglenoid process present [1]. (Warren & Black, 1985; Jupp & Warren, 1986)

145. Preglenoid process: labial side of surangular with straight dorsal margin anterior to glenoid [0]; forming dorsal projection well above the level of the glenoid articulation [1].

146. Arcadian groove running vertically on the posterior end of the PGA dividing the surangular: absent [0]; arcadian groove present [1]. (Warren & Black, 1985; Jupp & Warren, 1986)

147. Anterior Meckelian foramen: absent [0]; single anterior Meckelian foramen [1]; two or more anterior Meckelian foramina [2]. (Jupp & Warren 1986; Witzman, 2013)

148. Posterior Meckelian foramen: bordered by the prearticular, postsplenial and the angular [0]; posterior Meckelian foramen bordered by the prearticular and postsplenial exclusively [1]; posterior Meckelian foramen bordered by the prearticular and angular [2]. (Jupp & Warren 1986).

149. Length of the posterior Meckelian foramen: greater than 50% of the length of the adductor fossa [0]; length of the posterior Meckelian foramen less than a 50% of the length of the adductor fossa [1]. (Marsicano et al., 2017).

150. Parasymphysial foramina: on both sides of the symphysis absent [0]; parasymphysial foramina present [1]. (modified from Bolt & Lombard, 2001).

151. Chorda tympani foramen: located on the suture between the articular and the prearticular [0]; chorda tympanic foramen located on the prearticular alone [1]; chorda tympani foramen absent [2]. (Jupp & Warren, 1986).
152. Chorda tympani foramen: enlarged [0]; not enlarged [1]. (Marsicano et al. 2017).
153. Labial wall of adductor fossa: nearly horizontal [0]; strongly convex dorsally [1].
154. Glenoid fossa: above level of dentary tooth row [0]; below or at the level of dentary tooth row [1]. (Bolt & Lombard, 2001).
155. Prearticular hamate process: absent [0]; hamate process present on the anterior margin of the glenoid fossa above the level of the dorsal surfaces of the surangular and articular 24 [1]. (Damiani, 2001).
156. Adsymphisial bone: absent [0]; present [1]. (Bolt & Lombard, 2001).
157. Prearticular: extends anteriorly to contact the anterior coronoid [0]; retracted until the level of the midpoint of the middle coronoid [1]; prearticular does not extend anterior beyond the level of the suture of the middle and posterior coronoids [2]; prearticular extends anteriorly to reach the symphysis [3]. (modified from Ruta & Bolt, 2006)
158. Prearticular: not extending posterior to the level of the glenoid [0]; prearticular extending posterior to the glenoid, at least covering the medial face of the articular below the glenoid fossa [1]; prearticular extending on the lingual surface of the PGA [2]. (Warren & Marsicano, 2000).
159. Prearticular-surangular contact: absent [0]; present [1]. (Bolt & Lombard, 2001; Ruta & Bolt, 2006).
160. Prearticular-splenial contact: present [0]; absent [1]. (Ruta & Bolt, 2006).
161. Postsplenial mesial lamina: absent [0]; present [1]. (Bolt & Lombard, 2001; Ruta & Bolt, 2006).
162. Angular mesial lamina: absent [0]; present [1]. (Bolt & Lombard, 2001; Ruta & Bolt, 2006).
163. Ventral margin of angular: smoothly curved [0]; nearly flat for most of its length [1]. (Ruta & Bolt, 2006)

164. Posterior coronoid: not visible in labial view [0]; visible in labial view [1]. (Yates & Warren, 2000).

165. Parasymphysial teeth: behind the marginal tooth row [0]; parasymphysial teeth absent [1]. (Yates & Warren, 2000).

166. Parasymphysial fangs: present [0]; absent [1]. (Ruta & Bolt, 2006).

167. Lateral notch for reception of premaxillary fangs on the dentary: absent [0]; present [1]. (Bolt & Lombard, 2001; Ruta & Bolt, 2006).

168. Coronoid denticles: all three coronoids bear a field of small denticles [0]; field of denticles restricted to the posterior coronoid [1]; coronoids without any denticle fields [2]. (Yates & Warren, 2000).

169. Coronoid teeth: without teeth other than denticles [0]; posterior coronoid with a row of teeth [1]; all coronoids with a continuous tooth row [2]; anterior coronoid with a row [3]. (modified from Yates & Warren, 2000).

170. Coronoid fangs on the coronoids: present on all three coronids [0]; restricted to the anterior coronoid [1]; absent [2].

171. In lateral aspect, maximun depth of angular: subequal to smaller than maximun depth of the surangular [0]; greater than maximun depth of the surangular [1]. (Bolt & Lombard, 2001; Ruta & Bolt, 2006).

172. In lateral aspect, the labial surface of the post-glenoid area formed mainly by the angular and with the surangular located latero-dorsally: absent [0]; present [1].

173. Angular foramen on the contact between angular and prearticular, at the level of the glenoid: present [0]; absent [1]. (Bolt & Lombard, 2001).

174. Splenial contribution to the symphysis: present [0]; absent [1]. (Bolt & Lombard, 2001).

175. Splenial ventrolateral exposure: conspicuous [0]; barely visible [1]. (Bolt & Lombard, 2001).

176. Splenial mesial lamina: not expanding anterosposteriorly [0]; expanding anterosposteriorly, thus forming a wedge-like nearly triangular sheet of bone [1]. (Bolt & Lombard, 2001).

177. In mesial aspect, rearmost portion of splenial: closer to posterior margin of the symphysis [0]; closer to the anterior margin of the adductor fossa [1]. (Bolt & Lombard, 2001).
178. Anterior coronoid bulges medially from the lingual surface of the mandible: absent [0]; present [1].
179. Unsculpture dorsal strip on labial surface of dentary: absent [0]; present [1]. (Ruta & Bolt 2008).
180. Coronoid-splenial contact: absent [0]; present [1]. (Bolt & Lombard, 2001).
181. Middle coronoid-splenial contact: absent [0]; present [1]. (Bolt & Lombard, 2001).
182. Glenoid fossa: with hooked posterodorsal process, causing glenoid to face anterodorsally [0]; shallow fossa facing mostly dorsally [1].
183. Dentary teeth: same size as maxillary teeth [0]; much larger than maxillary teeth [1]. (modified from Clack et al., 2012).
184. Dentition of the adsymphyseal bone: fangs [0]; tooth row [1]; absent [2]. (modified from Bolt & Lombard, 2001).
185. Coronoid tooth row, if present: larger than marginal teeth [0]; equal to marginal teeth [1]; smaller than marginal teeth [2].
186. Dental material on prearticular: present [0]; absent [1]. (modified from Bolt & Lombard, 2001).
187. Dentary-postdentary suture: continuous, straight or with gradual curve [0]; strongly stepped in posterior third of suture [1].
188. Dentary-postdentary contact: "chamfered" overlap by dentary of postdentary bones [0]; firmly attached [1].
189. Mandibular lateral line canal: enclosed by postdentary bones for at least part of its length [0]; open for entirety of its length [1]; absent [2].
190. Meckelian bone exposure on medial surface of lower jaw: present for at least 30% of lower jaw length [0]; absent [1].
191. Free ventral lamina of splenial/postsplenial: present [0]; absent [1].

Postcranial skeleton

192. Posterior margin of the interclavicle: does not form a parasternal process [0]; forms a parasternal process [1]. (Ruta & Bolt, 2006).

193. Interclavicle wider than long (excluding parasternal process, if present): absent [0]; present [1]. (Ruta & Bolt, 2006).

194. Clavicles: presence of a suture between the anteroventral plates [0]; absent [1]. (Ruta & Bolt, 2006).

195. Distinct supinator process of the humerus projecting anteriorly from the distal portion of the anterior surface of the humerus shaft: absent [0]; present [1]. (Ruta & Bolt, 2006).

196. Iliac blade: with nearly parallel margins [0]; iliac blade flared proximally [1]. (Holmes at el., 1998).

197. Iliac blade: posteriorly inclined [0]; nearly vertical [1]. (Yates & Warren, 2000).

198. Ventral edges of adjacent intercentra: in contact [0]; prevented from contact by intervening pleurocentra [1]. (Yates & Warren, 2000).

199. Presacral intercentra: open dorsally (crescentic) [0]; at least some intercentra form a complete disc [1].

200. Presacral count: less than 30 vertebrae [0]; more than 30 vertebrae [1].

201. Broad posterior flanges projecting from at least some trunk ribs: absent [0]; present [1]. (Clack & Finney 2005; Ruta & Bolt, 2006).

202. Cleithrum: ossified [0]; unossified [1].

203. Cleithrum: large dorsal expansion along dorsal edge of scapular process [0]; mostly aligned with anterior border of scapula [1].

204. Postbranchial lamina of the cleithrum: present [0]; absent [1].

205. Scapular blade: tall and narrow [0]; low and broad [1].

206. Coracoid: ossified [0]; unossified [1].

207. Coracoid foramen: present [0]; absent [1].

208. Supraglenoid foramen: present [0]; absent [1].

209. Glenoid fossa: faces mostly posteriorly [0]; faces mostly laterally [1].

210. Number of digits in manus: 6 or more [0]; 5 [1]; 4 [2]; 3 or fewer [3].

211. Prepectoral plate of humerus: present [0]; absent [1].

212. Deltoid tubercle: absent [0]; present [1].

213. Entepicondylar foramen: present [0]; absent [1].

214. Entepicondylar process: large, broad, and squared-off [0]; weakly-developed expansion of the distal humerus [1].

215. Ectepicondylar process: strongly developed [0]; weakly-developed or absent [1].

216. Iliac blade: separate dorsal and posterior processes [0]; unipartite [1].

217. Adductor blade of femur: well-developed "adductor blade" more than half the length of the femur [0]; "adductor blade" reduced to a wea ridge, or absent [1].

c) Comments on Clack et al. (2019) phylogenetic analysis and results

To test whether our finding that *Gaiasia* is a stem tetrapod was due to convergence artefacts within our novel dataset, we scored *Gaiasia* into the phylogenetic treatment of Clack et al. (2019), a dataset built to examine the phylogenetic relationships of the problematic early tetrapod *Acherontiscus calendoniae.* This matrix (see Supplementary Datasets) is relatively large (260 characters, 57 taxa), extensively samples Devonian and Carboniferous early tetrapods, and shares significant character and taxon overlap with the majority of recent phylogenetic analyses of early tetrapod phylogeny. In addition to adding scores for *Gaiasia*, we added scores for three dvinosaur temnospondyls: *Trimerorhachis insignis*, *Acroplous vorax*, and *Dvinosaurus* spp. We ran two analyses of this dataset (see Supplementary Datasets). First, we conducted a maximum parsimony analysis in PAUP using the heuristic search with 10,000 random addition sequence. Due to significant computational burden of this analysis we ended the search at 1036 addition sequence replicates as new random addition replicates had ceased to find shorter trees. Our search recovered 7408 equally parsimonious trees of length 1412. In strict consensus, *Gaiasia* falls out into a broad polytomy with other Mississippian stem-group tetrapods. Our majority rule consensus shows that a plurality of these trees place *Gaiasia* close to *Koilops* from the Tournaisian of Scotland, stemward of baphetids and colosteids. Interestingly, we fail to recover dvinosaurs with other temnospondyls; dvinosaurs are resolved as the sister taxon of adelospondyls in a majority of MPTs but are not found closely-related to *Gaiasia*. We then re-ran our analyses applying a strong concavity constraint (Goloboff fit, K=10) to counteract the effects of highly-convergent characters on the resulting topology. We found only two MPTs (score=-195.10487). In both trees, *Gaiasia* is found to be the sister taxon of *Koilops*, stem-ward of most Carboniferous tetrapods and distinct from temnospondyls. We continue to find support for temnospondyl diphyly in this analysis, suggesting that this is a broader artefact of this dataset. We note some differences in the constitution of the tetrapod stem between our matrix and the matrix modified from Clack et al. (2019), notably the stem-tetrapod position of embolomeres in our dataset, and the more crownward position of

colosteids relative to baphetids in Clack et al. (2019); it is not clear to us whether this is a consequence of different approaches to character sampling, broader sampling of highly-incomplete taxa by Clack et al. (2019), or some other cause. We consider this further evidence of a Mississippian stem-tetrapod origin of the lineage leading to *Gaiasia*. This also reinforces recent findings that the phylogeny of early tetrapods remains highly labile.

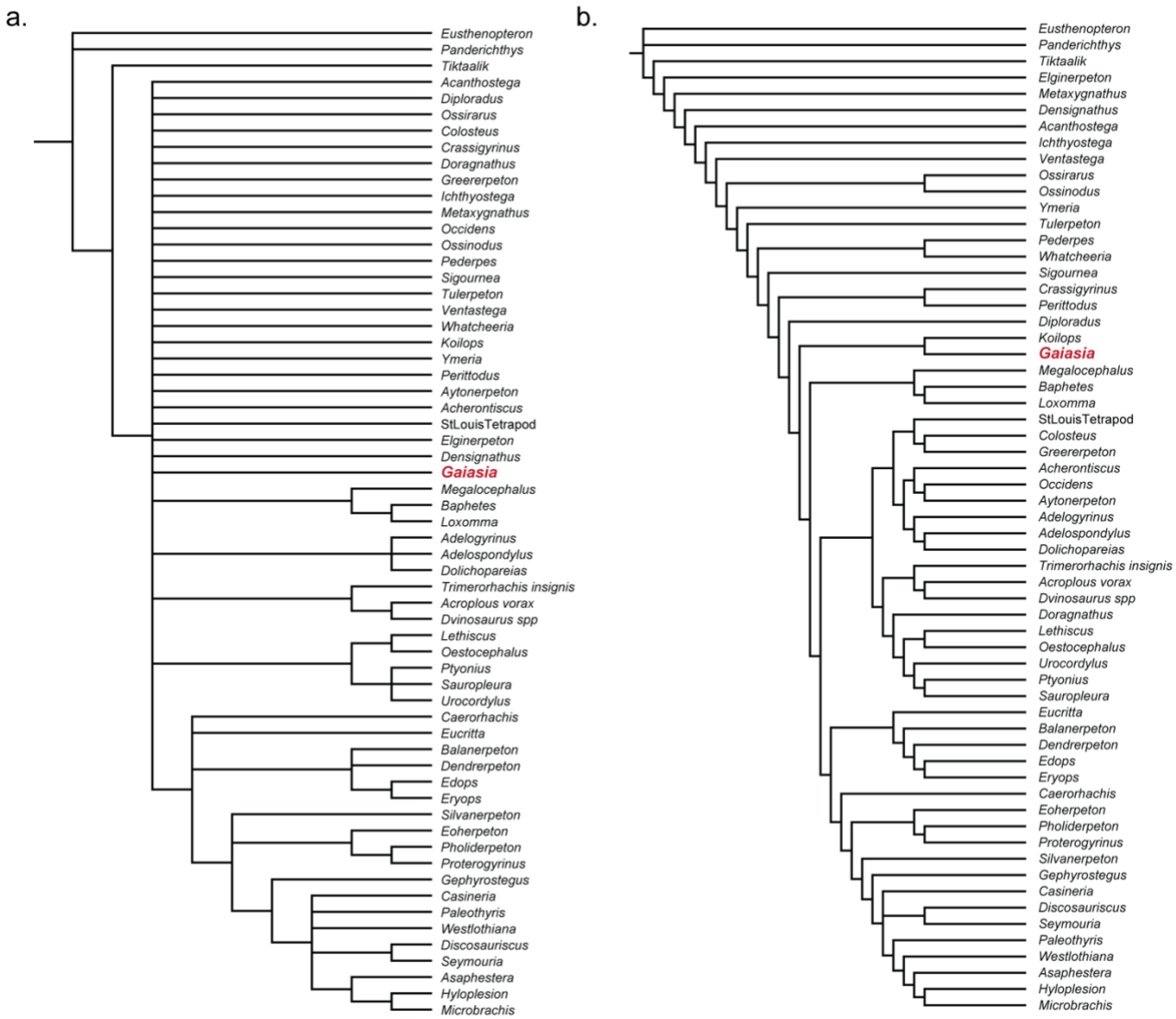

Figure S7. Strict consensus of 7408 equally parsimonious trees from the unweighted parsimony analysis (a), and strict consensus of two equally parsimonious trees from the implied weighting scheme (k=10) in (b)

3) Supplementary Tables 1 and 2

Taxon	Earliest Member	Locality	Age	Reference
Amniota	*Hylonomus lyelli*	Joggins, Nova Scotia, Canada. Joggins Formation, Cumberland Group	Earliest Pennsylvanian (Bashkirian)	Carroll (1964)
Stereospondyli	*Australerpeton cosgriffi*	Serro do Cadeado, Brazil. Serrinha Member, Rio do Rasto Formation	Middle Permian (Roadian)	Francischini et al. (2018)
Archegosauridae	*Archegosaurus decheni*	Germany. Odernheim Horizon, Mesenheim Formation, Lower Rotliegend	Early Permian (Sakmarian)	Boy (1987)
Dvinosauria	*Saurerpeton (Isodectes) obtusum*	Mazon Creek, Illinois. Francis Creek Shale	Pennsylvanian (Moscovian)	Milner (1982)
Eryopoidae	*Glaukerpeton avinoffi*	Pitcairn, Pennsylvania, USA. Glenshaw Formation, Conemaugh Group	Pennsylvanian (earliest Kasimovian)	Werneburg & Berman (2012)
Edopoidea	*Procochleosaurus jarrowensis*	Jarrow Colliery, Ireland.	Early Pennsylvanian (Bashkirian-Moscovian, Westphalian B)	Sequeira (1996)
Baphetida	*Spathicephalus marsdeni*	Fife, Scotland. Anstruther Formation, Strathclyde Group	Mississippian (Visèan)	Smithson et al. (2017)
Adelospondyli	*Palaeomolgophis scoticus*	Broxburn, West Lothian, Scotland. Pumpherson Oil Shale, Lower Oil Shale Group	Mississippian (Visèan)	Andrews & Carroll (1991)
Aïstopoda	*Lethiscus stocki*	Wardie Shore, Scotland. Lower Oil Shale Group	Mississippian (middle Visèan)	Wellstead (1982)
Whatcheeriidae	Becco Whatcheeriid	Becco, Belgium. Crupet Member, Evieux Formation	Upper Devonian (Fammenian)	Olive et al. (2016)

Table S1. First occurrences of higher clades in Text Figure 2.

Taxon	Earliest Gondwanan Member	Earliest Gondwanan Locality	Age	Reference
Amniota	*Mesosaurus*	Paraná Basin, Brazil. Irati Formation.	Early Permian (Artinskian)	Ventura Santos et al. (2006)
Stereospondyli	*Australerpeton cosgriffi*	Serro do Cadeado, Brazil. Serrinha Member, Rio do Rasto Formation	Middle Permian (Roadian)	Francischini et al. (2018)
Archegosauridae	*Prionosuchus plummeri*	Pastos Bons and Nazaria (multiple localities), Brazil. Pedra de Fogo Formation.	Latest early Permian (Kungurian?)	Cisneros et al. (2015)
Dvinosauria	*Timonya annae*, *Procuhy nazariensis*	Timon and Nazaria (multiple localities), Brazil. Pedra de Fogo Formation.	Early Permian (Kungurian?)	Cisneros et al. (2015)
Edopoidea	*Nigerpeton ricqlesi*	West of Arlit, Niger. Moradi Formation	Latest Permian	Steyer et al. (2006)

Table S2. First Gondwanan occurrences of higher clades in Text Figure 2.

4) Supplementary references

Alonso-Zarza, A.M. 2003. Palaeoenvironmental significance of palustrine carbonates and calcretes in the geological record. *Earth-Science Reviews* 60, 261–298.

Andrews, S. M., Carroll, R. L. 1991. The order Adelospondyli: Carboniferous lepospondyl amphibians. *Earth and Environmental Science Transactions of the Royal Society of Edinburgh* 82, 239–275.

Bolt, J. R., Lombard, R. E. 2001. The mandible of the primitive tetrapod *Greererpeton*, and the early evolution of the tetrapod lower jaw. *Journal of Paleontology* 75, 1016–1042.

Boucot, A.J., Xu, C., Scotese, C.R., Morley, R.J. 2013. Phanerozoic paleoclimate: an atlas of lithologic indicators of climate (Vol. 11). Tulsa, SEPM (Society for Sedimentary Geology).

Boy, J. A. 1987. Die Tetrapoden-Lokalitaten des saarpfalzischen Rotliegenden (?Ober-Karbon–Unter-Perm; SW-Deutschland) und die Biostratigraphie der Rotliegend-Tetrapoden. *Mainzer geowissenschaftliche Mitteilungen* 16, 31–65.

Boy, J. A. 1990. Uber einige Vertreter der Eryopoidea (Amphibia: Temnospondyli) aus dem europaischen Rotliegend (?hochstes Karbon – Perm). 3. Onchiodon. *Palaontologische Zeitschrift*, 64, 287–312.

Bystrow A.P., Efremov J.A. 1940. [*Benthosuchus sushkini* Efremov – a labyrinthodont from the Eotriassic of the Sharzenga River.] *Trudy Paleontologicheskogo Instituta* 10, 1–152 [In Russian].

Carroll, R. L. 1964. The earliest reptiles. *Zoological Journal of the Linnean Society* 45, 61–83.

Cisneros, J. C., Marsicano, C., Angielczyk, K. D., Smith, R. M., Richter, M., Fröbisch, J., Sadleir, R. W. 2015. New Permian fauna from tropical Gondwana. *Nature communications*, 6, 8676.

Clack, J. A., Ahlberg, P. E., Blom, H., Finney, S. M. 2012. A new genus of Devonian tetrapod from North-East Greenland, with new information on the lower jaw of Ichthyostega. *Palaeontology* 55, 73–86.

Clack, J. A., Ruta, M., Milner, A. R., Marshall, J. E., Smithson, T. R., Smithson, K. Z. 2019. *Acherontiscus caledoniae*: the earliest heterodont and durophagous tetrapod. *Royal Society open science*, 6(5), 182087.

Damiani, R. 2001. A systematic revision and phylogenetic analysis of Triassic mastodonsauroids (Temnospondyli: Stereospondyli). *Zoological Journal of the Linnean Society* 133, 379–482.

Francischini, H., Dentzien-Dias, P., Guerra-Sommer, M., Menegat, R., Santos, J. O. S., Manfroi, J., Schultz, C. L. 2018. A middle Permian (Roadian) lungfish aestivation burrow from the Rio do Rasto Formation (Paraná Basin, Brazil) and associated U-Pb dating. *Palaios* 33, 69–84.

Gierlowski-Kordesch, E.H. 1998. Carbonate deposition in an ephemeral siliciclastic alluvial system: Jurassic Shuttle Meadow Formation, Newark Supergroup, Hartford Basin, USA. *Palaeogeography, Palaeoclimatology, Palaeoecology* 140, 161–184.

Gubin, Y. M. 1986. New data on the archegosauroids of the East European Platform. *Paleontological Journal* 20, 70–5.

Holmes, R. R. 2000. Palaeozoic temnospondyls. In Heatwole, H., Carroll, R. L. (eds) *Amphibian Biology 4: Palaeontology*, 1082–120. Chipping Norton: Surrey Beatty

Holmes, R. B., Carroll, R. L., Reisz, R. R. 1998. The first articulated skeleton of *Dendrerpeton acadianum* (Temnospondyli, Dendrerpetontidae) from the Lower Pennsylvanian locality of Joggins, Nova Scotia, and a review of its relationships. *Journal of Vertebrate Paleontology* 18, 64–79.

Horsthemke, E. 1992. *Fazies der Karoosedimente in der Huabregion, Damaraland, NW-Namibia*. Gottinger Arb. Geol. Paliiont., 55, 102 pp.

Jupp, R., Warren A. A. 1986. The mandibles of the Triassic temnospondyl amphibians. *Alcheringa* 10, 99–124.

Lambiase, J. J. 1989. The framework of African rifting during the Phanerozoic. *Journal of African Earth Sciences* 8, 183–190.

Marsicano, C. A., Warren, A. 1998. The first Palaezoic rhytidosteid: *Trucheosaurus major* (Woodward, 1909) from the late Permian of Australia, and a reassessment of the Rhytidosteidae (Amphibia, Temnospondyli). *Bull. Nat. Hist. Mus. Lond*. (Geol.) 54, 147–154.

Marsicano, C. A., Latimer, E., Rubidge, B., Smith, R. M. 2017. The Rhinesuchidae and early history of the Stereospondyli (Amphibia: Temnospondyli) at the end of the Palaeozoic. *Zoological Journal of the Linnean Society* 181, 357–384.

Milner, A. R. 1982. A small temnospondyl amphibian from the Lower Pennsylvanian of Nova Scotia. *Journal of Paleontology*, 1302–1305.

Milner, A. R. 1990. The radiations of temnospondyl amphibians. Pp. 321–349 in P. D. Taylor & G. P. Larwood (eds) *Major Evolutionary Radiations*. Clarendon Press, Oxford.

Milner, A. R., Sequeira, S. E. K. 1994. The temnospondyl amphibians from the Visean of East Kirkton, West Lothian, Scotland. *Transactions of the Royal Society of Edinburgh, Earth Sciences* 84, 331–361.

Milner, A. R., Sequeira, S. E. K. 1998. A cochleosaurid temnospondyl amphibian from the Middle Pennsylvanian of Linton, Ohio, USA. *Zoological Journal of the Linnean Society* 122, 261–290.

Olive, S., Ahlberg, P. E., Pernègre, V. N., Poty, É., Steurbaut, É., Clément, G. 2016. New discoveries of tetrapods (ichthyostegid-like and whatcheeriid-like) in the Famennian (Late Devonian) localities of Strud and Becco (Belgium). *Palaeontology* 59, 827–840.

Pardo, J. D., B. J. Small, Huttenlocker, A. K. 2017a. Stem caecilian from the Triassic of Colorado sheds light on the origins of Lissamphibia. *Proceedings of the National Academy of Sciences of the United States of America* 114, E5389–E5395.

Pardo, J. D., Szostakiwskyj, M., Ahlberg, P. E., Anderson, J. S. 2017b. Hidden morphological diversity among early tetrapods. *Nature* 546(7660), 642–645.

Romer, A. S., Witter, R. V. 1942. *Edops*, a primitive rhachitomous amphibian from the Texas red beds. *The Journal of Geology* 50, 925–960.

Ruta, M., Bolt, J. R. 2006. A reassessment of the temnospondyl amphibian *Perryella olsoni* from the Lower Permian of Oklahoma. *Transactions of the Royal Society of Edinburgh Earth Sciences* 97,113–165.

Santos, R.V., Souza, P.A., Alvarenga, C., Dantas, E.L., Pimentel, M.M., de Oliveira, C. G. de Araújo, L.M. 2006. Shrimp U–Pb zircon dating and palynology of bentonitic layers from the Permian Irati Formation, Paraná Basin, Brazil. *Gondwana Research* 9, 456–463.

Schäfer, W. 1972. *Ecology and Palaeoecology of Marine Environments*. The University of Chicago Press, Chicago

Schoch, R.R. 2013. The evolution of major temnospondyl clades: an inclusive phylogenetic analysis. *Journal of Systematic Palaeontology* 11, 673–705.

Sequeira, S. E. K. 1996. A cochleosaurid amphibian from the Upper Carboniferous of Ireland. In Milner, A. R. (ed.) *Studies on Carboniferous and Permian Vertebrates*. Special Papers in Palaeontology 52, 65–80.

Sequeira, S. E. K. 1998. The cranial morphology and taxonomy of the saurerpetontid *Isodectes obtusus* comb. nov. (Amphibia: Temnospondyli) from the Lower Permian of Texas. *Zoological Journal of the Linnean Society* 122:237–259.

Sequeira, S. E. K. 2004. The skull of *Cochleosaurus bohemicus* Fric, a temnospondyl from the Czech Republic (Upper Carboniferous) and cochleosaurid interrelationships. *Transactions of the Royal Society of Edinburgh, Earth Sciences* 94, 21–43.

Shishkin, M. A. 1973. The morphology of the early Amphibia and some problems of lower tetrapod evolution. Trudy *Paleontologiceskogo Instituta Akademiya Nauk SSSR*, 137, 1–257. [In Russian]

Smithson, T. R., Browne, M. A., Davies, S. J., Marshall, J. E., Millward, D., Walsh, S. A., Clack, J. A. 2017. A new Mississippian tetrapod from Fife, Scotland, and its environmental context. *Papers in Palaeontology* 3, 547–557.

Steyer, J. S., Damiani, R., Sidor, C. A., O'Keefe, F. R., Larsson, H. C., Maga, A., Ide, O. 2006. The vertebrate fauna of the Upper Permian of Niger. IV. *Nigerpeton ricqlesi* (Temnospondyli:

Cochleosauridae), and the edopoid colonization of Gondwana. *Journal of Vertebrate Paleontology* 26, 18–28.

Stollhofen, H., Stanistreet, J.G., Rohn-Davies, R., Holzforster, F. Wanke, A. 2000. The Gai-As lake system, northern Namibia and Brazil. In: Gierlowski-Kordesch, E.H. and Kelts, K. (eds.) *Lake basins through space and time*. Mem. Am. Assoc. Petrol. Geol. 46, 87–108.

Tankard, A. J., M. A. Uliana, H. J. Welsink, V. A. Ramos, M. Turk, A. B. França, E. J. Milani, B. B. de Brito Neves, N. Eyles, J. Skarmeta, H. Santa Ana, F. Wiens, M. Cirbián, O. López Paulsen, G. J. B. Germs, M. J. De Wit, T. Machacha, R. McG. Miller. 1995. Structural and tectonic controls of basin evolution in southwestern Gondwana during the Phanerozoic. In: A. J. Tankard, R. Suarez-Soruco, and H. J. Welsink (eds.) *Petroleum Basins of South America*: AAPG Memoir 62, 5–52.

Van Hinsbergen, D.J.J., De Groot, L.V., Van Schaik, S.J., Spakman, W., Bijl, P.K., Sluijs, A. 2015. A paleolatitude calculator for paleoclimate studies. *PLoS ONE 10*, e0126946, 1–21.

Wanke, A., Stollhofen, H., Lorenz, V. 2000. Unconformities in the Karoo sediments in NW-Namibia and their tectonic implications. *Communs Geol. Surv. Namibia* 12, 291–301

Warren A. A., Black, T. 1985. A new rhytidosteid (Amphibia: Labrinthodontia) from the Early Triassic Arcadia Formation of Queensland, Australia, and the relationships of Triassic temnospondyls. *Journal of Vertebrate Paleontology* 5, 303–327.

Warren, A., Marsicano, C. A. 2000. A phylogeny of the Brachyopoidea (Temnospondyli, Stereospondyli). *Journal of Vertebrate Paleontology* 20, 462–483.

Watson, D. M. S. 1962. The evolution of the labyrinthodonts. *Philosophical Transactions of the Royal Society of London B* 245, 219–265.

Wellstead, C. F. 1982. A Lower Carboniferous aïstopod amphibian from Scotland. *Palaeontology* 25, 193–208.

Werneburg, R., Berman, D. S. 2012. Revision of the aquatic eryopid temnospondyl *Glaukerpeton avinoffi* Romer, 1952, from the Upper Pennsylvanian of North America. *Annals of Carnegie Museum* 81, 33–60.

Werner, M. 2006. *The stratigraphy, sedimentology and age of the Late Palaeozoic Mesosaurus Inland Sea, SW-Gondwana: new implications from studies on sediments and altered pyroclastic layers of the Dwyka and Ecca Group (lower Karoo Supergroup) in southern Namibia*. Unpublished PhD Thesis, University of Würzburg, Germany, 428pp.

Williams, C.A., Krause, F.F. 1998. Pedogenic–phreatic carbonates on a Middle Devonian (Givetian) terrigenous alluvial–deltaic plain, Gilwood Member (Watt Mountain Formation), northcentral Alberta, Canada. *Sedimentology* 45, 1105–1124.

Witzmann, F. 2013. Phylogenetic patterns of character evolution in the hyobranchial apparatus of early tetrapods. *Transactions of the Royal Society of Edinburgh: Earth Sciences* 104: 145–167.

Yates, A. M., Warren, A. A. 2000. The phylogeny of the 'higher' temnospondyls (Vertebrata: Choanata) and its implications for the monophyly and origins of the Stereospondyli. *Zoological Journal of the Linnean Society* 128, 77–121.